Motor Current Signature Analysis to Detect Static Eccentricity in Case of 300 kW Induction Motor

Saleh Elawgali*

Department of Electrical and Electronics Engineering
Faculty of Engineering, Sirte University
E-mail: elawgali@su.edu.ly

Abstract

In this paper the current spectrums of a five pole-pairs, 300 kW, squirrel cage induction motor were calculated for the cases of full symmetry and static eccentricity.
The calculations account for variable inductances affected by slotting and eccentricity. The calculations were followed by Fourier analysis of the stator currents in steady state operation.
The paper includes stator current spectrums affected by different degrees of static eccentricity to demonstrate the effect of static eccentricity on the stator current spectrum and to predict the harmonics related to this ailment. The motor under investigation represents a special example because its stator current spectrum includes more than one slot harmonic that is, supposedly, due to the unique configuration of the stator winding and rather high number of pole pairs (p=5). Zooms of the current spectrums, around the 50 Hz fundamental harmonic as well as of each slot harmonic zone, are included. In addition the paper includes the stator current spectrum that referred to the real measured currents.

Keywords: Induction machine, diagnostics, current spectrum, harmonics.

1. Introduction

Large 3-phase induction motors are used in power stations to drive main auxiliaries such as cooling water pumps, fans and boiler feed pumps. The sudden failure of a main auxiliary drive can result in loss of prime generating capacity at critical times with consequent substantial cost penalties.

It would be beneficial therefore to have some form of online monitoring for such motors to detect incipient troubles and enable planned preventive maintenance or repair to be carried

*Author for correspondence

out. Planned maintenance strategies and machine condition monitoring have, of course, been used in power stations for many years to ensure motor failures are kept to a minimum. In general, this has been successful but there is always the possibility of a failure due to a fault which is difficult to detect even with existing monitoring techniques. An example of this is a rub between the rotor and stator which can result in serious damage to the stator core and windings. The fundamental cause may be due to overall bearing movement, rotor flexing due to dynamic disturbances, use of narrow air gaps for high efficiency, or stator core movement [1]. To prevent a rub due to such a variety of conditions requires a monitoring strategy for the online detection of air gap eccentricity and other malfunctions such as drive misalignment, dynamic imbalance changes, broken rotor bars and inter turn faults in the stator windings.

The importance of this paper is that it is trying to specify the spectrum harmonics as an indication to static eccentricity based on the analysis of the stator currents, in order to predict the fault in an earlier stage to prevent any sudden failure of the machine

2. A Review of Diagnostic Techniques

Several contributions can be found in the literature dealing with the performance analysis of induction motors under eccentricity conditions [1-15]. The Winding Function Approach (WFA) is a useful technique for modeling an induction motor under these conditions, which accounts for all the space harmonics in the machine. Multiple coupled circuit model [2, 3] enables the dynamic modeling of induction motors with both arbitrary winding layout and/or unbalanced operating conditions. Hence, this model has found application in the analysis of asymmetrical fault conditions in machines such as rotor failures, stator winding faults, or air gap eccentricity [4, 5, 6].

Fault-specific signals are also present in the electromagnetic flux which can be measured by coils sensing the axial leakage flux [7]. Instantaneous power signature analysis is also used. The single-phase instantaneous power was proposed for the diagnosis of mixed rotor faults [8]. The signal-based methods commonly use the stator current as a measurement since it is sensitive to the rotor faults, and it is a suitable method to obtain a diagnostic

index and a threshold stating the edge between faulty and healthy conditions.

Conventional motor current signature analysis (MCSA) techniques based on the frequency analysis of the stator current are currently the most common and well-established methods. In fact, MCSA is simple and effective under suitable operating conditions. As an example, MCSA is the optimal choice for electrical machines under steady-state conditions and rated load [4, 6, 9].

3. *Air Gap Eccentricity*

Air gap eccentricity takes two basic forms: static and dynamic. Static eccentricity is characterized by a displacement of the axis of rotation where the position of the minimal air gap length is fixed in space, Fig. 1 a. It can be caused by the stator ovality or by the incorrect positioning of the rotor or stator at the commissioning stage. Since the rotor is not centered within the stator bore, the field distribution in the air gap is no longer symmetrical. The non-uniform air gap gives rise to a radial force of electromagnetic origin, called unbalanced magnetic pull (UMP), which acts in the direction of minimum air gap. However, static eccentricity may cause dynamic eccentricity, too [1]. The latter means that the rotor is not rotating on its own axis and the minimum air gap rotates with the rotor, Fig. 1 b. This kind of eccentricity may be caused by a bent shaft, mechanical resonances, bearing wear or misalignment or even static eccentricity as mentioned above. Therefore, the non-uniform air gap of a certain spatial position is sinusoidally modulated and results in an asymmetric magnetic field, too. This, accordingly, gives rise to a revolving UMP [8].

The combined static and dynamic eccentricity is called mixed eccentricity [2]. In this condition, both rotor and rotation axes are displaced with respect to the stator one, which results in more complicated geometry condition of the motor compared to the two other cases for its modelling. Air gap eccentricity in induction machines causes characteristic harmonic components in electrical, electromagnetic, and mechanical quantities. Therefore, either mechanical quantities such as vibrations or torque oscillations or electrical quantities such as currents or instantaneous power can be analyzed to detect eccentricity conditions [8].

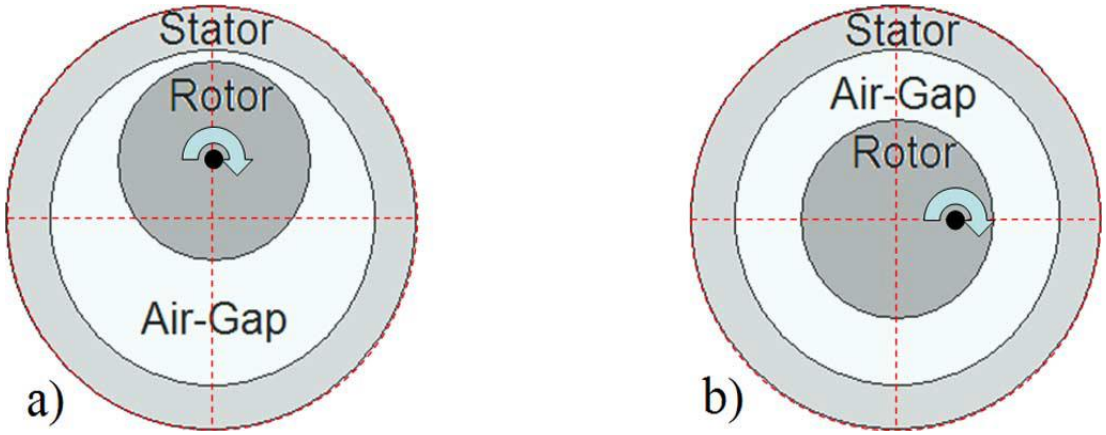

Figure 1. Air Gap Eccentricity, a) Static Eccentricity, b) Dynamic Eccentricity

4. Simulation Results

The calculations presented in this paper are based on the poly-harmonic model accounting for static and dynamic eccentricity, stator and rotor slotting, parallel branches as well as cage asymmetry [16, 17]. The model is based on purely numerically calculated inductances in order to quantitatively account for all interactions between eccentricities and slotting.

The coefficients of inductances were calculated numerically, assuming that the main or air gap flux may be separated from the leakage flux (as it is well established in the theory of electrical machines) [18]. The leakage inductances are calculated in, a roughly, classical way. The main inductances are calculated via division of the air gap into small channels, down which the main magnetic flux passes from the stator to the rotor and vice versa. The lengths of these channels depend on eccentricity and slotting and they are modified for several hundred positions of the rotor.

The elementary contributions of the flux, of each channel, are then summed up in accordance with actual configuration of the stator windings.

The rotor is modelled as a set of meshes constituted by adjacent cage bars and end ring segments. The dependence of inductances on the rotor angle allows calculation of their

derivatives, necessary for calculation of the torque in the next program performing numerical integration of differential equations.

In this paper the calculations are performed with a special software owned by the Chair of Electrical Machines, AGH University of Science and Technology, Krakow, Poland.

The program for dynamics simulation consists of four base classes [17]:

- Class Pa1 calculates mainly leakage inductances.
- Class In16 calculates self and mutual main inductances accounting for true stator winding configuration as well as for slotting and eccentricity.
- Class De18 calculates derivatives of the inductances, with respect to rotor angle.
- Class Dy20 performs integration of differential equations using 3D matrices of inductances and their derivatives stored on the disk by class De18.

The spectral analysis was performed by program Sp1 that calculates Fast Fourier Transform (FFT) as well as least squares approximation of the fundamental component of the stator currents.

The calculations performed are referred to a 300 kW squirrel-cage induction motor, with 5-pole pairs (p=5) and N_S/N_R = 72/88 of stator/rotor slots. All spectrums refer to steady state operation by full loading torque TL = 7050 Nm.

- **IV- a). Healthy Machine**

As a reference basis, the calculations were performed for fully symmetrical machine. The full spectrum of the stator line current is shown in fig. 2.

In addition to the 50 Hz fundamental harmonic, the spectrum contains the following slot harmonics:

1. The first slot harmonic $Slh_{1,}$ of the frequency of about 823.5 Hz, in the first slot harmonic zone. Its amplitude is about -38 dB.
2. The second slot harmonic $Slh_{2,}$ of the frequency of about 1797 Hz, in the second slot harmonic zone. Its amplitude is about -72.5 dB.
3. The main slot harmonic $Slh_{,}$ of the frequency of about 4417 Hz, in the main slot harmonic zone. Its amplitude is about -70 dB.

The frequency of the main slot harmonic, Slh, can be predicted by the following formula [19]:

$$f_{Slh} = \left| f_1 + h \cdot NR(1-s)n_s \right| \quad (1)$$

Where: the supply frequency f_1 = 50 Hz, the parameter h = 5 [16], the no. of rotor slots NR = 88, the slip s = 0.0074318, and the synchronous speed $n_s = f_1/p$ = 10 revolutions per second.

In the above equation, the parameter h represent the order of the main slot harmonic zone, so if h = 1 that means the first slot harmonic zone is the main one whereas h =2 means the second slot harmonic zone is the main one. For more details see [16].

Also, the frequency of the first slot harmonic, Slh_1, can be predicted by the following formula [19]:

$$f_{Slh1} = \left| f_1 - h' \cdot NR(1-s)n_s \right| \quad \text{, where the parameter } h' = 1 \text{ [16].} \quad (2)$$

Whereas, the frequency of the second slot harmonic, Slh_2, can be predicted by the following formula [19]:

$$f_{Slh2} = \left| f_1 + h'' \cdot NR(1-s)n_s \right| \quad \text{, where the parameter } h'' = 2 \text{ [16].} \quad (3)$$

It is clear, from the stator current spectrum fig. 2, that this machine, of five pole pairs (p = 5), possess slot harmonics other than the main slot harmonic, even for the fully symmetrical case.

Supposedly, this is due to the unique configuration of the stator winding and rather high number of pole pairs for this machine.

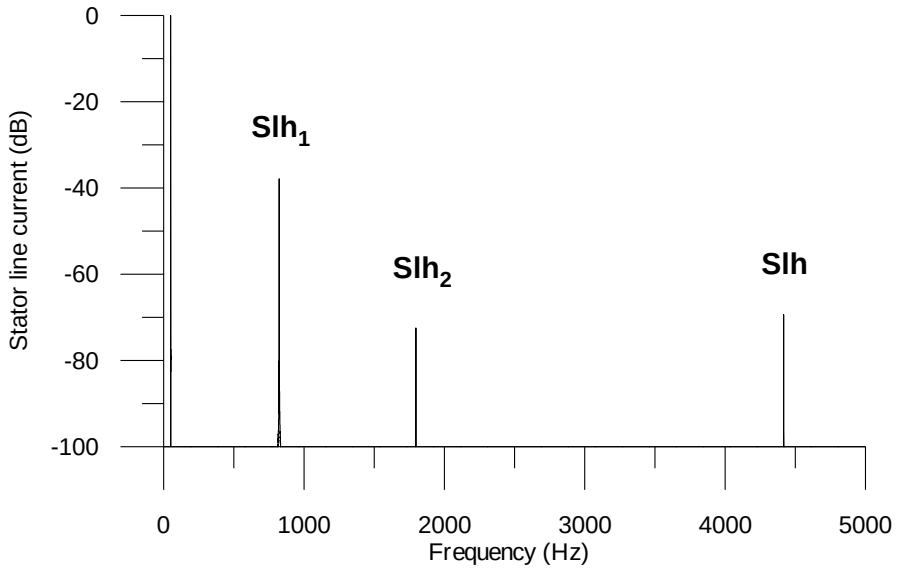

Figure 2. Spectrum of the calculated stator current (full symmetry)

- **IV- b). Static Eccentricity**

In this case the calculations performed considering that the rotor axis is shifted by a certain value of the geometrical air gap thickness toward the first coil group of the stator phase A [2, 5].

The stator line current spectrum of fig. 3a refers to the case of 50% static eccentricity.

The spectrum contains a pair of harmonics in the first, second and main slot harmonic zones, as compared to just the first, second and main slot harmonics in the case of full symmetry, fig 2. Each pair consist of the slot and the twin harmonics.

The zoom of the first slot harmonic zone is shown in fig. 3b. It contains the first slot harmonic Slh_1 of the frequency of about 823.5 Hz, as well as the first twin harmonic tw_1, of the frequency of abut 923.5 Hz, which is spaced by about 100 Hz to the right of the first slot harmonic Slh_1.

The first twin harmonic is present in a very conspicuous manner, reaching the level of about -54 dB, what delivers clear evidence for the static eccentricity in this case.

The frequency of the first twin harmonic, tw_1, to the right of the first slot harmonic, Slh_1, can be predicted by the following formula [19]:

$$f_{tw1} = \left| f_1 + h^{'} \cdot NR(1-s)n_s \right| \quad \text{, where the parameter } h^{'} = 1 \text{ [16].} \qquad (4)$$

The zoom of the second slot harmonic zone is shown in fig. 3c. It contains the second slot harmonic Slh_2 of the frequency of about 1797 Hz, as well as the second twin harmonic tw_2, of the frequency of abut 1697 Hz, which is spaced by about 100 Hz to the left of the second slot harmonic Slh_2.

The amplitude of the second twin harmonic is smaller (-82 dB), as compared to the first one, but it also gives additional evidence for the static eccentricity.

The frequency of the second twin harmonic, tw_2, to the left of the second slot harmonic, Slh_2, can be predicted by the following formula [19]:

$$f_{tw2} = \left| f_1 - h^{''} \cdot NR(1-s)n_s \right| \quad \text{, where the parameter } h^{''} = 2 \text{ [16].} \qquad (5)$$

The zoom of the main slot harmonic zone is shown in fig. 3d. It contains the main slot harmonic Slh of the frequency of about 4417 Hz, as well as the twin harmonic tw, of the frequency of abut 4317 Hz, which is spaced by about 100 Hz to the left of the main slot harmonic Slh.

It should be noted that the amplitude of the twin harmonic tw trespasses the amplitude of the main slot harmonic Slh, reaching the level of about -62 dB. That gives additional confirmation for the presence of the static eccentricity in this case. The frequency of the twin harmonic, tw, to the left of the main slot harmonic, Slh, can be predicted by the following formula [19]:

$$f_{tw} = \left| f_1 - h \cdot NR(1-s)n_s \right| \quad \text{, where the parameter } h = 5 \text{ [16]} \qquad (6)$$

On the whole, we conclude that the presence of the twin harmonics in the first, second and main slot zones delivers clear evidence for the static eccentricity, but it should be noted that the first slot zone is the most important one for the diagnostic purposes.

However, the main slot zone is out of our interest, because the frequencies of the harmonics in this zone are out of the frequency range of the available current registrations, amounting for the time been to 3000 Hz (sampling frequency is 6000 Hz).

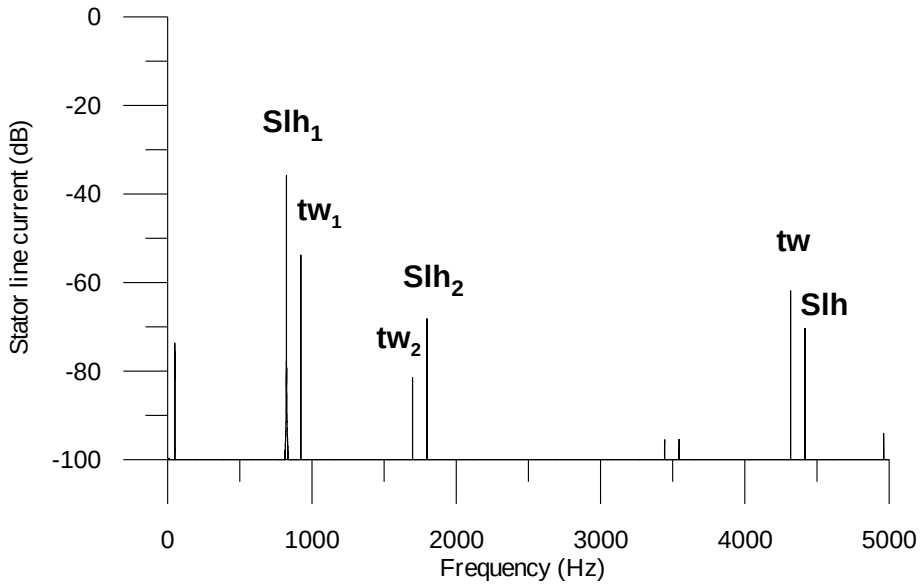

Figure 3a Spectrum of the calculated stator current (50% static eccentricity)

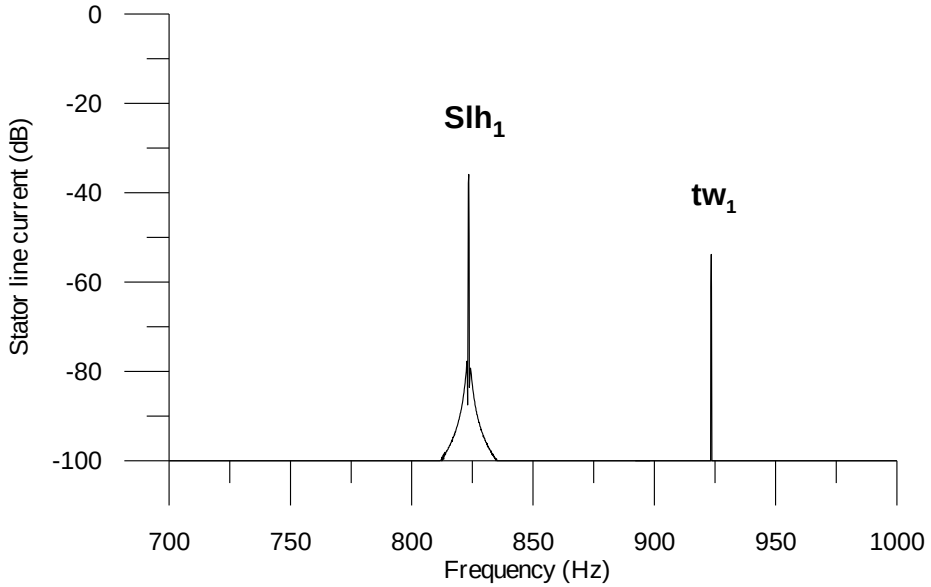

Figure 3b. Zoom of the first slot harmonic zone (50% static eccentricity)

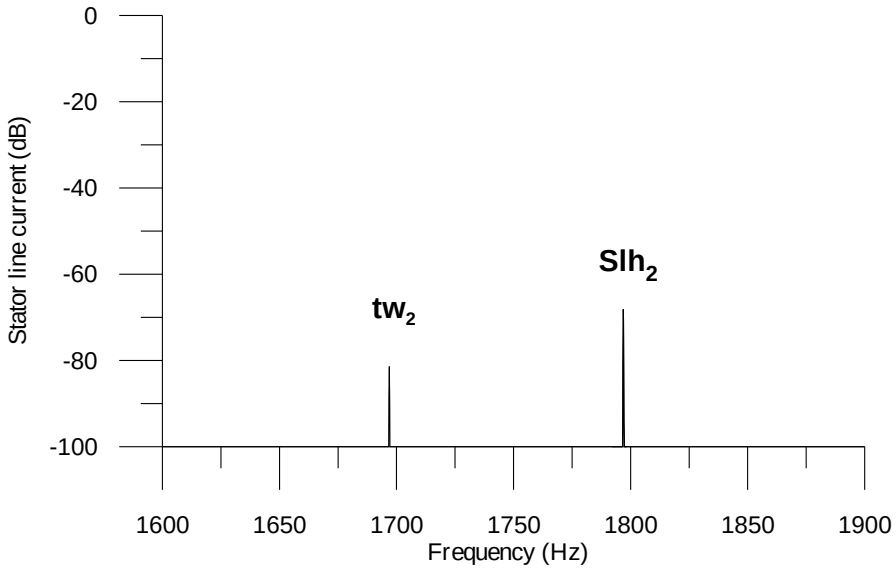

Figure 3c. Zoom of the second slot harmonic zone (50% static eccentricity)

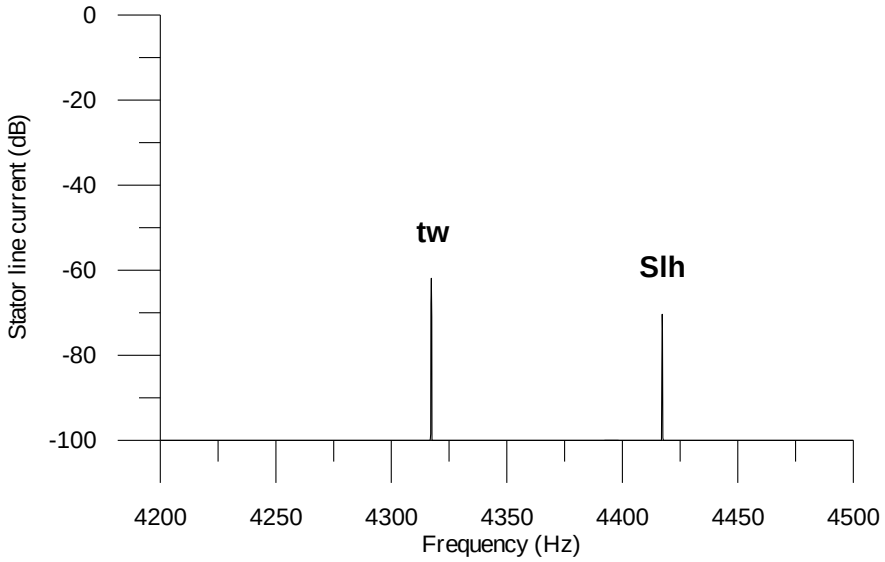

Figure 3d. Zoom of the main slot harmonic zone (50% static eccentricity)

In order to demonstrate the sensitivity of the twin harmonic amplitude to the degree of static eccentricity, the calculations were performed also for the cases of 60% and 70% static eccentricity.

The spectrum of fig. 4 refers to the case of 60% static eccentricity. In this spectrum the twin harmonics are clearly visible to the right of the first slot harmonic Slh_1, to the left of the second slot harmonic Slh_2 as well as to the left of the main slot harmonic Slh.

Generally, the amplitudes of all these twin harmonics magnified, as compared to the previous case of 50 % static eccentricity.

As for the first slot harmonic zone, which is the most important one for the diagnostic purposes, the first twin harmonic tw_1 is very conspicuous, reaching the level of about -50 dB.

Similarly, the spectrum of fig. 5 referring to the case of 70% static eccentricity, contains again all the twin harmonics as in the previous cases of 50% and 60% static eccentricity.

The amplitude of the first twin harmonic, tw_1, to the right of the first slot harmonic, Slh_1, magnified. It is now of about -46 dB. That proves the sensitivity of the twin harmonic to the changes of the static eccentricity degree, and allows for relying on this harmonic as a good indication for the existence of the static eccentricity.

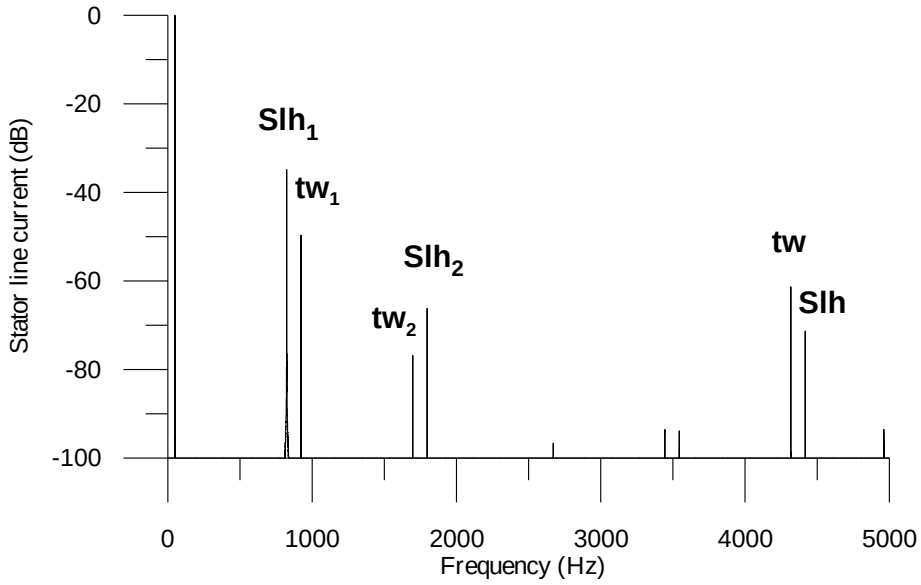

Figure 4 Spectrum of the calculated stator current (60% static eccentricity)

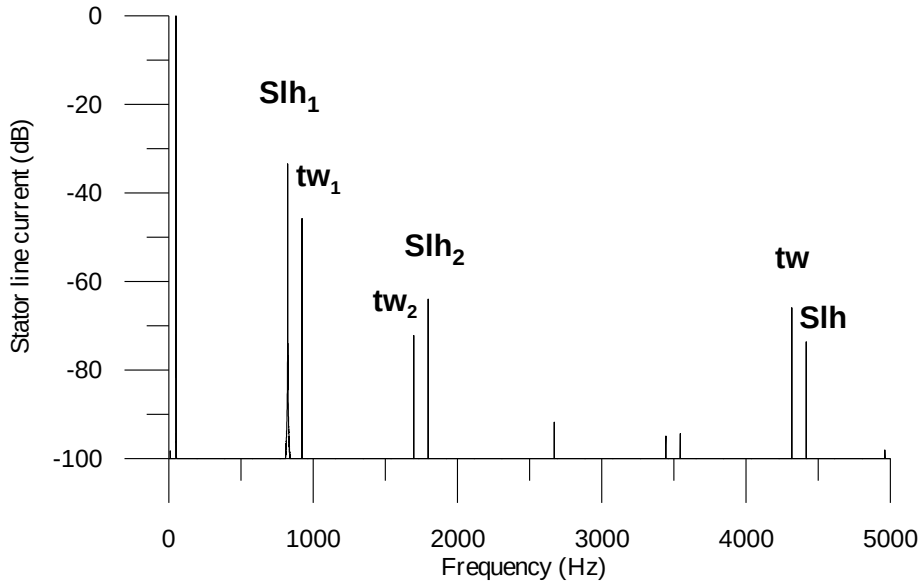

Figure 5. Spectrum of the calculated stator current (70% static eccentricity)

5. Measurement Results

Spectral analyses were performed for a number of currents really registered in the industry. Many registered currents have been analyzed, which referred to the five pole pair, 300 kW, induction machines, labeled in the industry as WS, among all the cases analyzed, there were some cases found to show up some static eccentricity.

In the following there is an example of the really measured stator current. The full spectrum of fig. 6a refers to the WS, 300 kW induction machine, (file name 4WS1U2). The presence of the first twin harmonic tw_1, to the right of the first slot harmonic Slh_1, as shown in fig. 6c, it delivers clear evidence for the static eccentricity in this case. Hence, this case was classified as showing up pure static eccentricity.

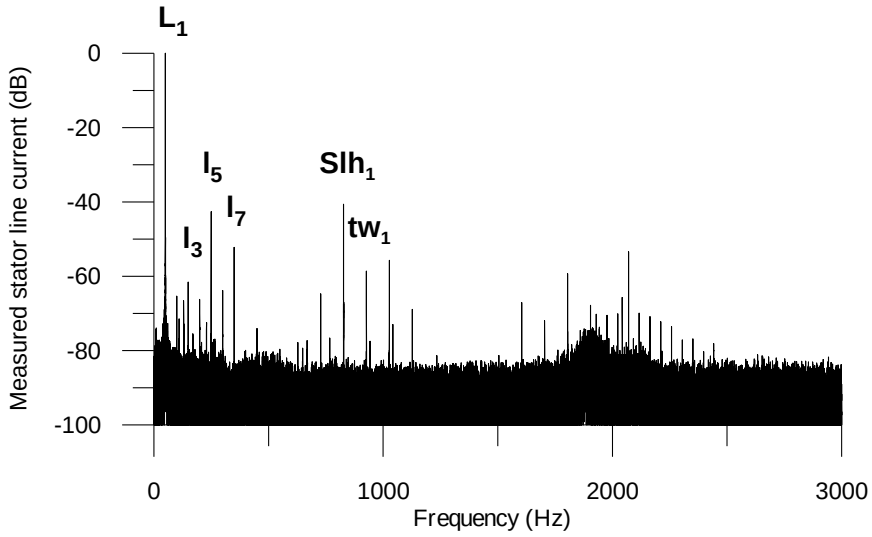

Figure 6a. Spectrum of the measured stator current (4WS1U2)

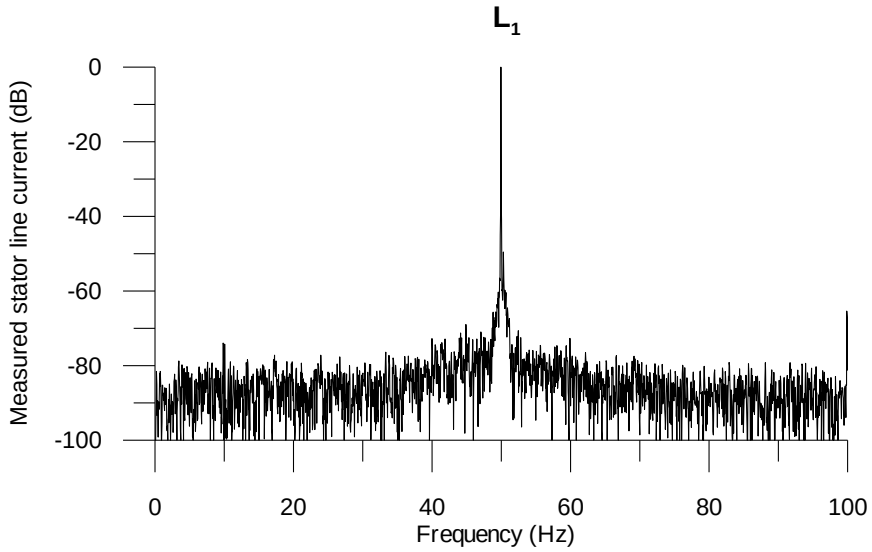

Figure 6b. Zoom around 50 Hz of the measured stator current (4WS1U2)

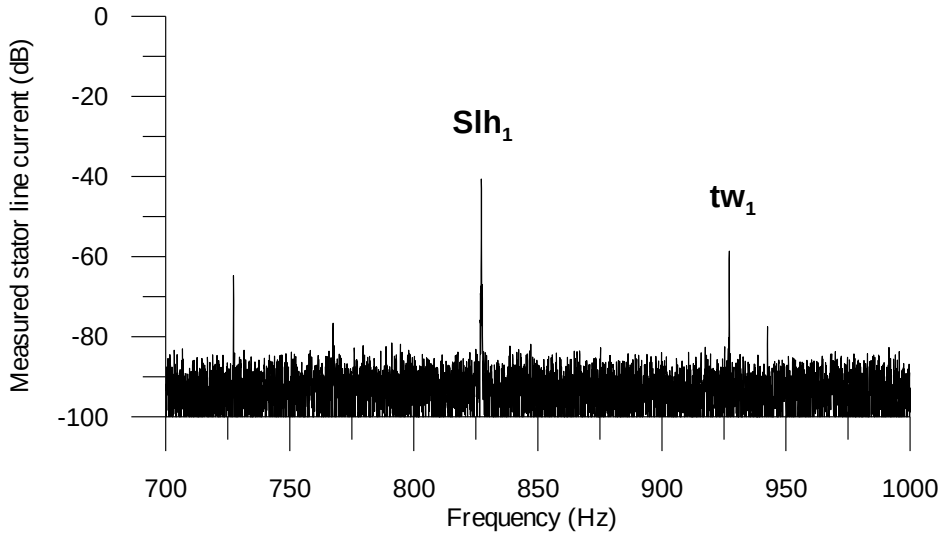

Figure 6c Zoom of the first slot harmonic zone of the measured stator current (4WS1U2)

6. Conclusion

1. The presence of the twin harmonic in the first, second and main slot harmonic zones gives clear indication for the existence of the static eccentricity.
2. Each pair of harmonics, in the above mentioned slot harmonic zones, is consist of the slot harmonic which is always present, independently of the static eccentricity, and the twin harmonic which gives an evidence for the static eccentricity.
3. The calculations proved that the main and first slot harmonic zones are, from diagnostic point of view, the most important ones, as they contain diagnostic information, in form of the most important diagnostic harmonics. In addition, the slot zones are cleaner as compared to the fundamental harmonic zone, normally polluted by many other harmonics
4. The amplitude of the twin harmonic is affected positively by the degree of static eccentricity.
5. The coincidence between measured and calculated current spectrums proved the effectiveness of this diagnostic procedure for diagnosing static eccentricity in an induction motors.

6. Quantitative calculations deliver solid base for reliable diagnosis of induction machines and differentiating between different ailments.

7. References

[1] Cameron, J. R., Thomson, W. T. and Dow, A. B., "*Vibration and Current Monitoring for Detecting Air-gap Eccentricity in Large Induction Motors*", IEEE Proceedings, Vol. 133, pt B, No. 3, May 1986, pp. 155-163.

[2] Devanneaux, V., Kabbaj, H., Dagues, B., and Faucher, J., "*An Accurate Model of Squirrel Cage Induction Machines Under Static, Dynamic or Mixed Eccentricity*", IEEE International Symposium on Diagnostics for Electric Machines, Power Electronics and Drives, SDEMPED, 1-3 September 2001, Grado-Italy, pp. 121-126.

[3] Joksimovic, G. M.; Duvoric, M.; Penman , J.; Arthur N.:*Dynamic simulation of dynamic eccentricity in induction machines - Winding Function Approach.* IEEE Trans. On Energy Conversion, vol. 15, n° 2, June, 2000, pp. 143-148.

[4] Thomson, W. T., "*On-Line Current Monitoring to Diagnose Shaft Misalignment in Three-Phase Induction Motor Drive Systems*", International Conference on Electrical Machines, ICEM'94, 5-8 September 1994, Paris, France, pp. 238-243.

[5] Thomson, W. T. and Barbour, A. "*On-Line Current Monitoring and Application of A Finite Element Method to Predict the Level of Static Air-Gap Eccentricity in Three-Phase Induction Motors*", IEEE Transaction on Energy Conversion, Vol. 13, No. 4, December 1998, pp. 347-354.

[6] Thomson, W. T. and Finger, M., "*Current Signature Analysis to Detect Induction Motor Faults*", IEEE Industry Applications Magazine, July/August 2001, pp. 26-34.

[7] Dorrell, D.; Thomson, W.; Roach, S. "*Analysis of airgap flux, current and vibration signals as a function of the combination of static and dynamic airgap eccentricity in 3-phase induction machines*". Conf. Rec. IEEE-IAS Annu. Meeting, 1995, pp. 563-570.

[8] M'hamed Drif, A. J. Marques Cardoso "*Airgap Eccentricity Fault Diagnosis, in Three-Phase Induction Motors, by the Complex Apparent Power Signature Analysis*" IEEE, International Symposium on Power Electronics, Electrical Drives, Automation and Motion, SPEEDAM 2006, 1-4244-0194-1/06/$20.00 ©2006 IEEE, pp. S35, 18-22

[9] Humberto Hen AO, Gerard-Andre Capolino, Manes Fernandez-Cabanas, Fioren Zo filippetti, Claudio Bruzzese, Elias Strangas, Remus Pusca, Jorge Estima, Martin Riera-Guasp, and Shahin Hedayati-Kia, " *Trends in Fault Diagnosis for Electrical Machines*", IEEE industrial electronics magazine, June 2014 ■ IEEE 1932 4529/14©2014, PP. 31-42.

[10] Bellini, A., Filippetti, F., Franceschini, G. and Tassoni, C. "*Towards Correct Quantification of Induction Machines Broken Bars Through Input Electrical Signals*", International Conference on Electrical Machines, ICEM'2000, 28-30 August 2000, Espoo, Finland, pp. 781-785.

[11] Bellini, A., Filippetti, F., Franceschini, G. and Tassoni, C., "*Quantitative Evaluation of Induction Motor Broken Bars by Means of Electrical Signature Analysis*", IEEE, Transactions on Industry Applications, Vol. 37 No. 5, 2001, pp. 1248-1255.

[12] Bangura, J., F., Povinelli, R., J., Demerdash, N., A., and Brown, R., H., "*Diagnostics of Eccentricities and Bar/End-Ring Connector Breakages in Poly-phase Induction Motors Through a Combination of Time-Series Data Mining and Time-Stepping Coupled FE-State-Space Techniques*", IEEE Transactions Industry Applications, Vol. 39, No. 4, July/August 2003, pp. 1005-1013.

[13] Duque, O., Perez, M. and Morinigo, D., "*Practical Application of the Spectral Analysis of Line Current for the Detection of Mixed Eccentricity in Cage Induction Motors Fed by Frequency Converter*", International Conference on Electrical Machines ICEM'2004, 5-8 September 2004, Cracow, Poland, pp. 823-824.

[14] Stavrou, A., Penman, J., "*The On-Line Quantification of Air-Gap Eccentricity in Induction Machines*", International Conference on Electrical Machines, ICEM'94, 5-8 September 1994, Paris, France, pp. 261-266.

[15] Swedrowski, L., Rusek, J., "*Model and Simulation Test of a Squirrel-Cage Induction Motor with Oscillation of the Air Gap*", IEEE International Symposium on Diagnostics for Electric Machines, Power Electronics and Drives, SDEMPED, 7-9 September 2005, Vienna, Austria, pp. 131-136.

[16] Rusek, J. "*Categorization of Induction Machines Resulting from Their Harmonic-Balance Model*", Electromagnetics, Vol. 23, No. 3, April 2003, Taylor & Francis, pp. 277-292.

[17] Rusek, J. "*Computer Implementation of Induction Machine Dynamical Model Accounting for Broken Bars, Eccentricities, Slotting and Parallel Branches*", International Conference on Electrical Machines, ICEM'2000, 28-30 August 2000, Espoo, Finland, pp. 868-872.

[18] Rusek, J. "*Reflection of Eccentricities in Spectral Composition of Currents of Induction Machines*" International Conference on Electrical Machines, ICEM'96, 10-12 September 1996, Vigo, Spain, pp. 470-475.

[19] Rusek, J. "*Category, Slot harmonics and the Torque of Induction Machines*", The International Journal for Computation and Mathematics in Electrical and Electronic Engineering, COMPEL, Vol. 22 no. 2, 2003, pp. 388-409.